

Undercooling of bulk liquid silicon in an oxide flux

Y. Shao and F. Spaepen

Division of Applied Sciences, Harvard University, Cambridge, Massachusetts 02138

(Received 7 November 1995; accepted for publication 11 December 1995)

Drops of molten silicon surrounded by a SiO_2 -BaO-CaO flux were undercooled at 350 K below their melting temperature. This undercooling is 75 K greater than the largest one reported so far for bulk silicon. To account for this result as well as the nucleation data from laser-melted thin films, classical nucleation theory requires a crystal-melt interfacial tension with a positive temperature coefficient. © 1996 American Institute of Physics. [S0021-8979(96)05406-4]

INTRODUCTION

The undercooling of a melt below its thermodynamic crystallization temperature is often limited by the presence of impurities that act as heterogeneous crystal nucleants. It has been shown that surrounding the melt with a liquid flux can greatly increase the undercooling.^{1,2} It is thought that an effective flux eliminates nucleants from the surface or the bulk of the melt by dissolution or inclusion. Kui *et al.*² showed that a liquid B_2O_3 flux could be used to bypass the crystallization in a large mass of liquid $\text{Pd}_{40}\text{Ni}_{40}\text{P}_{20}$ entirely, so that it could be undercooled to its glassy state. Devaud and Turnbull³ used the same flux to undercool liquid Ge by as much as $\Delta T = 415$ K below the melting point ($T_M = 1210$ K); this corresponds to a relative undercooling, $\Delta T/T_M$, of 0.34. Similar results have been obtained by Lau *et al.*⁴ The same flux cannot be used with liquid Si, since Si reduces B_2O_3 ; attempts to use it gave no undercooling.⁵ The largest undercooling obtained for bulk liquid Si, using uncoated liquid droplets on a fused silica substrate, is 275 ± 20 K,⁶ which corresponds to a relative undercooling of 0.16. The structural similarities between silicon and germanium, for both their crystalline and liquid phases, make it likely that larger undercoolings should be obtainable in Si. A substantially larger undercooling would make it necessary to reassess the link made between the bulk undercooling and the undercooling in thin films following pulsed laser melting⁷ based on homogeneous crystal nucleation.⁸

EXPERIMENTS

A suitable flux for undercooling liquid silicon must meet two requirements: It must be chemically compatible with Si, and it must be sufficiently fluid at the undercooled temperatures. Pure molten SiO_2 , for example, even though it is chemically satisfactory, becomes too viscous below the melting temperature of Si, and attempts to use it as a flux have been unsuccessful.⁵ An extensive investigation of the alloys of chemically satisfactory oxides led to the identification of a suitable composition (in weight %): 47.5 SiO_2 ·13.5 CaO·39.0 BaO.

The flux was formed by heating the powdered constituents (from Johnson-Matthey; highest commercially available purity: SiO_2 : 99.9995%, CaO: 99.999% CaCO_3 , BaO: 99.9%) for 2 h at 1300 °C in a Pt crucible in air. Quenching, by removing the crucible from the furnace, produced a transparent glass. The first fluxes that were used had a light yel-

lowish color due to a 100 ppm Fe content (determined by inductively coupled plasma mass spectroscopy; introduced as 200 ppm trace impurity in the BaO). Replacing the BaO with purer BaCO_3 (99.997%) greatly reduced the Fe content. The glass softened around 1000 °C and became very fluid above 1300 °C.

The experiments were carried out in a stainless steel chamber. A small Ta box heater was clamped between two water-cooled electrodes. The flux and the Si chip (about 1 mm in diameter when melted, 99.9999% pure, from Johnson-Matthey) were put in a thin fused silica hemispherical shell, about 6 mm in diameter. The system was evacuated to 10 mTorr, and thoroughly purged with purified Ar, which was kept flowing very slowly at a slight overpressure during the experiment. A W-Re thermocouple was placed directly above the sample. The temperature was calibrated by melting several pure materials. The cooling rate in the experiment was maintained at 4 K/s. Melting and crystallization were observed through a window. Nucleation was marked by recalescence or by a change in reflectivity of the surface.

RESULTS

Of the 23 samples run, about half could be undercooled by more than 300 K, and 3 by as much as 350 K. These large undercoolings were observed in the both the Fe-free and Fe-containing fluxes.

Figure 1 shows an optical micrograph of the solidification morphology of a droplet undercooled by 350 K in the Fe-free flux. Note the presence of many solidification twins. There are also a number of small precipitates at the grain boundaries. Energy-dispersive x-ray analysis shows that they are Ba rich. Most likely, they are formed by rejection during solidification of a small amount of Ba dissolved in the liquid Si. A thermochemical computation shows that, although the formation energy of BaO is much greater than that of SiO_2 , the entropy of solution allows a small amount of Ba to be reduced and dissolved into liquid Si. Quantitative analysis of the micrograph shows that the amount of Ba dissolved in the melt is at most 0.16 at. %. Since the variation of the nucleation temperature (heterogeneous or homogeneous) with composition generally parallels the liquidus,⁹ a look at the Si-Ba phase diagram¹⁰ shows that the depression of the nucleation temperature due to the dissolved Ba is at most 4 K. A direct estimate, which may be more accurate given that

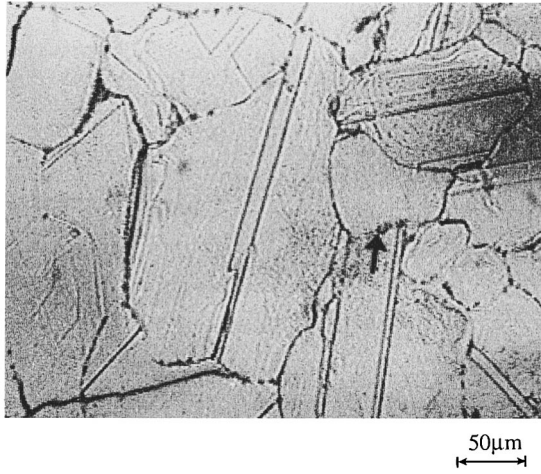


FIG. 1. Optical micrograph of the solidification product of molten silicon coated by an oxide flux, undercooled 350 K below the melting temperature. The arrow marks one of the Ba-rich precipitates at the grain boundary.

there is still some uncertainty about the experimental liquidus, is presented in Appendix A, and yields a depression of only 0.7 K.

DISCUSSION

The nucleation frequency associated with these observations can be estimated from the cooling rate ($T=4$ K/s), the volume of the sample ($V=4 \times 10^{-10}$ m³), and the nucleation temperature ($T_n=1335$ K). Appendix B describes the procedure, which gives a nucleation rate $I(T_n)=3.9 \times 10^9$ m⁻³ s⁻¹. This is plotted in Fig. 2, together with the nucleation rates estimated from earlier experiments on bulk⁶ or thin-film samples.^{7,11} The volume used in the calculations for the bulk undercooling experiments is that of the entire sample, not that of the individual grains in the solidification product. The

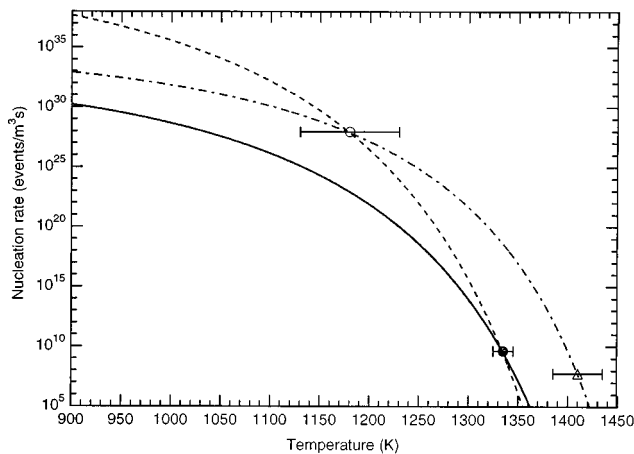


FIG. 2. Nucleation rates of silicon crystals from the melt derived from undercooling measurements. Open circle: laser-irradiated thin film (Ref. 7); triangle: uncoated bulk sample (Ref. 6); filled circle: oxide-coated bulk sample (this work). The lines are fits from classical nucleation theory. Solid curve: constant interfacial tension $\sigma=0.38$ J/m²; dot-dashed curve: constant interfacial tension $\sigma=0.34$ J/m²; dashed curve: temperature dependent interfacial tension with 1.46 interfacial layers and fitting parameters $\tilde{s}=S_i/\Delta S_f=-0.67$, $\tilde{h}=H_i/\Delta H_f=-0.32$.

latter procedure would increase $I(T_n)$ by about 10^4 . The choice was based on undercooling work on liquid Ge,^{3,4} which suggests that the individual grains result from fragmentation of the dendrite skeleton during growth following a single initial nucleation event. In the thin films (<1 μ m), there is less volume available for such a breakup,¹² and it is more plausible to use the volume of the individual grain for the calculation of $I(T_n)$, as was done in the analysis by Stiffler *et al.*⁷

In earlier work, the data at low and high temperature could be interpreted jointly by assuming that both represented homogeneous nucleation.⁷ In the classical theory, the nucleation frequency is given by

$$I=I_0 \exp\left(-\frac{16\pi}{3kT} \frac{\sigma^3}{\Delta G_v}\right), \quad (1)$$

where $I_0=10^{39}$ m⁻³ s⁻¹ is a prefactor determined by the jump frequency across the interface,^{13,15} σ is the crystal-melt interfacial tension, and ΔG_v is the difference in bulk free energy, per unit volume, between the two phases. As illustrated in Fig. 2, the data could be connected with a plot of Eq. (1), using a constant interfacial tension $\sigma=0.34$ J/m². The present experiments demonstrate that nucleation in the earlier bulk work⁶ was not homogeneous, since a substantially larger undercooling was obtained under similar conditions of volume and cooling rate. As Fig. 2 shows, a fit of Eq. (1) through the data from the present work, using $\sigma=0.38$ J/m², does not go through the data from the thin film work.

The only way the data can be reconciled with a homogeneous nucleation model is by assuming that the interfacial tension increases with temperature. A positive temperature coefficient for σ has been invoked in the interpretation of the data on homogeneous nucleation of Hg crystals from the melt.¹³ Such a coefficient reflects the lowered entropy resulting from the order induced in the first few liquid layers by the planar constraints of the crystal.^{14,15} As shown in Appendix C, the magnitude and temperature coefficient of σ required to fit both data in Fig. 2 can be accounted for by a uniform liquid interfacial layer, 1.46 monolayers thick, in which the entropy is lowered by $0.67 \Delta S_f$ and the enthalpy by $0.32 \Delta H_f$, where ΔS_f and ΔH_f are, respectively, the entropy and enthalpy of fusion.

Since the model has three parameters (the interfacial width δ , the interfacial entropy S_i , and the interfacial enthalpy H_i), and is fit to just two data points, one parameter had to be assigned based on structural considerations. Since the liquid Si in which the localization occurs is structurally similar to other metallic liquids, the interfacial thickness is taken to be the same as in the hard sphere model¹⁵⁻¹⁷ used to model the Hg interface. The remaining parameters are obtained from the fit. The entropy drop is similar to that in Hg ($0.68 \Delta S_f$), which is plausible, given the structural similarity between the two phases. The enthalpy drop is considerably larger than that in Hg ($0.10 \Delta H_f$). The difference in bonding between crystalline and liquid silicon makes an *a priori* estimate of the interfacial enthalpy difficult. Extrapolation of the temperature dependence of σ to the melting point of Si gives a value of 0.45 J/m².

Most likely the homogeneous nucleation limit has not been reached in the present experiments either. For example, the experiments in the Fe-containing flux produced small iron silicide precipitates around the droplet, and therefore probably also a thin iron silicide coating around it, which could act as a crystal nucleant. The temperature dependence of the interfacial tension is therefore probably stronger than the one calculated here, and the interfacial tension at the melting point should be considered a lower limit.

CONCLUSION

This work has demonstrated that bulk liquid silicon can be undercooled considerably further than had previously been achieved. This implies that homogeneous crystal nucleation did not occur in the earlier experiments; most likely, it did not occur in the present experiments either. The crystal-melt interfacial tension derived from the application of the classical theory for homogeneous nucleation is therefore a lower limit. A comparison of this value to that derived from experiments on laser-melted thin films of silicon indicates that the interfacial tension increases with temperature. The value of the positive temperature coefficient is also a lower limit. The observed temperature dependence can be accounted for by reasonable values of the interfacial entropy and enthalpy; the entropy drop in the liquid near the interface is similar to that in other metallic melts, such as mercury. Finally, the chemical stability and low viscosity of the new oxide flux developed in this work makes it potentially useful for the undercooling of high-temperature liquids other than silicon.

ACKNOWLEDGMENTS

We thank David Turnbull and Mike Aziz for valuable discussions. This work was supported by the National Aeronautics and Space Administration under Contract No. NAGW 2838.

APPENDIX A: DEPRESSION OF THE NUCLEATION TEMPERATURE DUE TO DISSOLVED IMPURITIES

Consider the nucleation of a pure silicon crystal from an ideal liquid solution containing an atomic fraction $x = 1 - x_{\text{Si}}$ of impurity. These are good approximations for an impurity with low solubility in crystalline Si, and for the chemical potential of the silicon solvent in a dilute liquid solution. The change in bulk free energy per unit volume upon formation of the nucleus is

$$\Delta G_v = \frac{1}{\bar{V}} (\mu_{\text{Si}}^l - \mu_{\text{Si}}^{c,o}), \quad (\text{A1})$$

where \bar{V} is the molar volume of crystalline Si, and μ_{Si}^l and $\mu_{\text{Si}}^{c,o}$ are the chemical potentials of silicon in, respectively, the liquid solution and the pure crystalline phases. In an ideal solution,

$$\mu_{\text{Si}}^l = \mu_{\text{Si}}^{l,o} + RT \ln(x_{\text{Si}}), \quad (\text{A2})$$

where $\mu_{\text{Si}}^{l,o}$ is the chemical potential of pure liquid Si, which can be related to that of pure crystalline Si at the same temperature by

$$\mu_{\text{Si}}^{l,o} = \mu_{\text{Si}}^{c,o} + \Delta S_f(T_M - T), \quad (\text{A3})$$

where ΔS_f is the entropy of fusion and T_M is the melting point of pure Si. Combining Eqs. (A1)–(A3) gives

$$\Delta G_v = \frac{1}{\bar{V}} (\Delta S_f(T_M - T) + RT \ln(x_{\text{Si}})). \quad (\text{A4})$$

For pure silicon

$$\Delta G_v = \frac{1}{\bar{V}} \Delta S_f(T_M - T). \quad (\text{A5})$$

In the classical nucleation theory, the nucleation rate at temperature T is

$$I = I_0 \exp \left[- \frac{16\pi}{3kT} \frac{\sigma^3}{\Delta G_v^2} f(\theta) \right], \quad (\text{A6})$$

where I_0 is a prefactor to the jump frequency across the interface, σ is the crystal-melt interfacial tension, and $f(\theta)$ is a geometrical factor that depends on the wetting angle θ of a heterogeneous nucleant. The nucleation temperature, T_n , is that at which I reaches a given value, and is determined by experiment. We are interested in the change in T_n as a result of the addition of a small amount of impurity to the melt. Equating the main temperature-dependent factor, $T\Delta G_v$, terms in Eq. (A6) for the two cases of Eqs. (A4) and (A5) gives

$$T_{n,0} [\Delta S_f(T_m - T_{n,0})]^2 = T_n [\Delta S_f(T_m - T_n) + RT_n \ln(x_{\text{Si}})]^2. \quad (\text{A7})$$

Using values appropriate for the present problem [$\Delta S_f = 30.03$ J/mol K; $x_{\text{Si}} = 1 - 0.0016$; $T_M = 1685$ K; $T_n = (1685 - 350) \text{ K} = 1335$ K], the equation can be solved easily for the difference between the two nucleation temperatures (keeping in mind that it is small), which yields $T_{n,0} - T_n = 0.7$ K.

APPENDIX B: DETERMINATION OF THE NUCLEATION RATE FROM OBSERVATIONS DURING CONTINUOUS COOLING

If in an isothermal experiment on a system of volume V , nucleation is observed at a time t , the steady-state nucleation rate, $I(T)$, can be estimated by stating that the probability of nucleation under these conditions, $I(T)Vt$, should be equal to unity.

Under the condition of continuous cooling at a rate \dot{T} , this condition is modified by breaking up the process into infinitesimal isothermal steps of duration $dt = dT/\dot{T}$ and integrating to get the total probability

$$\frac{V}{\dot{T}} \int_{T_M}^{T_n} I(T) dT = 1, \quad (\text{B1})$$

where T_M is the melting point, and T_n is the temperature at which the nucleation is observed (1335 K in this experiment). We are interested in estimating $I(T = T_n)$. The integral

is simplified by knowing that $I(T)$ increases very steeply with decreasing temperature, so that most of the value of the integral is accrued in a narrow temperature interval, ΔT , just above T_n . The condition then becomes

$$\frac{V}{\bar{V}} \int_{T_n - \Delta T}^{T_n} I(T) dT = 1. \quad (\text{B2})$$

According to the classical nucleation theory, the temperature dependence of the steady-state nucleation rate is

$$I(T) = I_0 \exp \left[- \frac{16\pi}{3kT} \frac{\sigma^3}{\Delta G_V^2} f(\theta) \right]. \quad (\text{B3})$$

The meaning of the parameters are the same as those in Appendix A. With ΔG_V given by

$$\Delta G_V = \frac{1}{\bar{V}} \Delta S_f (T_M - T), \quad (\text{B4})$$

where ΔS_f is the molar entropy change upon transformation and \bar{V} is the molar volume of the nucleating phase. Expansion to first order of all the temperature-dependent terms, which we take to include σ , in the integrand in a Taylor series around T_n gives

$$\frac{VI_0}{\bar{V}} \int_0^{\Delta T_{\max}} \exp[-B(1 + A\Delta T)] d(\Delta T) = 1, \quad (\text{B5})$$

where

$$A = \frac{3\sigma'_0}{\sigma_0} - \frac{1}{T_n} + \frac{2}{T_M - T_n} \quad (\text{B6})$$

and

$$B = \frac{16\pi}{3kT_n} \frac{\bar{V}^2 \sigma_0^3}{\Delta S_f^2 (T_M - T_n)^2} f(\theta). \quad (\text{B7})$$

σ_0 and σ'_0 are, respectively, the interfacial tension and its temperature derivative at T_n , and ΔT_{\max} is an arbitrary integration limit below which the integrand becomes negligible. Integration gives

$$- \frac{VI_0}{\bar{V}} \frac{1}{AB} \exp(-B) [\exp(-AB\Delta T_{\max}) - 1] = 1. \quad (\text{B8})$$

This can be simplified by recognizing that $I(T_n) = I_0 \exp(-B)$ or $B = \ln(I_0/I(T_n))$, and that for ΔT_{\max} sufficiently large $\exp(-AB\Delta T_{\max}) \ll 1$. The desired nucleation frequency is then

$$I(T_n) = AB \frac{\dot{T}}{\bar{V}}. \quad (\text{B9})$$

Iterative solution of this equation is fast, as can be seen from application to the present experiment.

In this case, $\dot{T} = 4$ K/s and the sample volume is $V = 4 \times 10^{-10}$ m³; theory gives $I_0 = 10^{39}$ m⁻³ s⁻¹ for condensed systems.¹³ Since the temperature dependence of the interfacial tension is not known *a priori*, we start by setting σ'_0 as zero. From the known values of T_M and T_n , the value $A = (201 \text{ K})^{-1}$ is computed. Since I_0 is an upper limit for $I(T_n)$, the upper limit for B is 94. This means that the upper limit for AB is 0.46. Using this as a first value in Eq. (B9)

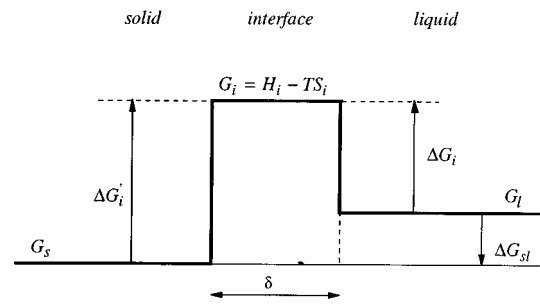


FIG. 3. Schematic illustration of the change of free energy per unit volume across a uniform crystal-melt interface below the melting temperature (from Ref. 15).

gives a starting estimate of $I(T_n) = 4.6 \times 10^9$ m⁻³ s⁻¹. This gives the new value $B = 67.5$. One more iteration gives $B = 67.86$, which in turn gives: $I(T_n) = 3.4 \times 10^9$ m⁻³ s⁻¹. This is accurate to two significant figures.

As discussed in the text, this value of $I(T_n)$ is compared to that obtained from pulsed laser melting experiments to obtain a temperature dependence of the interfacial tension. It is found that $\sigma'_0/\sigma_0 = (1472 \text{ K})^{-1}$. This gives, according to Eq. (B6) a new value $A = (143 \text{ K})^{-1}$. The iterative solution of Eq. (B9) using this new value is $I(T_n) = 3.9 \times 10^9$ m⁻³ s⁻¹.

Finally, we can estimate the temperature interval over which the integral is substantial. For the factor $\exp(-AB\Delta T_{\max})$ in Eq. (B8) to be greater than 0.1, use of the values of A and B from the last iteration shows that $\Delta T_{\max} < 4.9$ K, which is indeed a narrow temperature range. A calculation using the next term in the Taylor expansion showed that the higher order correction was entirely negligible.

In conclusion, given the insensitivity of A and B to variations in the experimental conditions, a useful order-of-magnitude estimate of the nucleation frequency in continuous cooling experiments is given by

$$I \left(\frac{\text{events}}{\text{m}^3 \text{ s}} \right) = \frac{1}{3(K)} \frac{\dot{T}(\text{K/s})}{V(\text{m}^3)}, \quad (\text{B10})$$

where the numerical prefactor is intermediate between those for a pulsed laser experiment and a bulk undercooling experiment.

APPENDIX C: FIT OF THE MODEL FOR THE TEMPERATURE DEPENDENCE OF THE INTERFACIAL TENSION TO THE NUCLEATION DATA

Figure 3 illustrates how the thermodynamic quantities in the model vary as a function of distance perpendicular to the interface.¹⁴ The interfacial tension is given by¹⁵

$$\tilde{\sigma} = \tilde{\delta} \left\{ \frac{1}{4} (\tilde{h} - \tilde{T}\tilde{s}) (\tilde{h} - \tilde{T}\tilde{s} - \tilde{T} + 1) \left[\sqrt{\tilde{h} - \tilde{T}\tilde{s}} + \sqrt{\tilde{h} - \tilde{T}\tilde{s} - \tilde{T} + 1} \right]^2 \right\}^{1/3}, \quad (\text{C1})$$

where the dimensionless quantities are defined as

$$\tilde{\sigma} = \frac{\sigma}{\lambda T_M \Delta S_f}, \quad \tilde{h} = \frac{\Delta H_i}{\Delta H_f}, \quad (C2)$$

$$\tilde{s} = \frac{\Delta S_i}{\Delta S_f}, \quad \tilde{T} = \frac{T}{T_M}, \quad \tilde{\delta} = \frac{\delta}{\lambda},$$

where λ is a characteristic atomic dimension (need not be specified), δ is the interfacial width, ΔS_i and ΔH_i are interfacial entropy and enthalpy differences per unit volume, which are defined in Fig. 3, and are assumed to be independent of temperature.

Since the model was developed for a constant atomic volume throughout the system, a molar volume of 11.67 cm^3 , the average of those of liquid and crystalline silicon, was used here.

Using Eq. (1), the interfacial tension at the two undercooled temperatures can be calculated from the nucleation frequencies determined by the method described in Appendix B: $\sigma(\tilde{T}_1=0.7)=0.34 \text{ J/m}^2$ and $\sigma(\tilde{T}_2=0.79)=0.38 \text{ J/m}^2$. Since Eq. (C1) has three fitting parameters, one needs to be determined from structural consideration. As for the analysis of the Hg data,¹⁵ the interfacial width, δ , is taken to be 1.46

monolayers. Using the interatomic distance of 2.50 \AA in liquid silicon,¹⁸ this gives $\delta=2.98 \text{ \AA}$. Equation (C1) for $\tilde{\sigma}(\tilde{T}_1)$ and $\tilde{\sigma}(\tilde{T}_2)$ can now be solved for the remaining quantities, which yields $\tilde{h} = -0.32$ and $\tilde{s} = -0.67$.

¹P. Bardenheuer and R. Bleckmann, *Stahl u. Eisen* **6**, 49 (1941).

²H. W. Kui, A. L. Greer, and D. Turnbull, *Appl. Phys. Lett.* **45**, 615 (1984).

³G. Devaud and D. Turnbull, *Mater. Res. Soc. Symp. Proc.* **57**, 89 (1986).

⁴C. F. Lau and H. W. Kui, *Acta Metall.* **39**, 323 (1991).

⁵G. Devaud, Ph.D. thesis, Harvard University, 1988.

⁶G. Devaud and D. Turnbull, *Appl. Phys. Lett.* **46**, 844 (1985).

⁷S. R. Stiffler, M. O. Thompson, and P. S. Peercy, *Phys. Rev. Lett.* **60**, 2519 (1988).

⁸P. V. Evans, G. Devaud, T. F. Kelly, and Y.-W. Kim, *Acta Metall.* **38**, 719 (1990).

⁹C. V. Thompson and F. Spaepen, *Acta Metall.* **31**, 2021 (1983).

¹⁰*Binary Alloy Phase Diagrams*, edited by T. B. Massalski (American Society for Metals, Metals Park, OH, 1986), Vol. 1.

¹¹The nucleation rates plotted in Fig. 2 are slightly different from those in Ref. 7 because they have been recalculated using the procedure of Appendix B.

¹²M. J. Aziz (private communication).

¹³D. Turnbull, *J. Chem. Phys.* **20**, 411 (1952).

¹⁴D. Turnbull, in *Physics of Non-Crystalline Solids*, edited by J. A. Prins (North-Holland, Amsterdam, 1964), p. 41.

¹⁵F. Spaepen, in *Solid State Physics*, edited by H. Ehrenreich and D. Turnbull (Academic, New York, 1994), Vol. 47, p. 1.

¹⁶F. Spaepen, *Acta Metall.* **23**, 729 (1975).

¹⁷F. Spaepen and R. B. Meyer, *Scripta Metall.* **10**, 257 (1976).

¹⁸Y. Kita, J. B. Van Zytveld, Z. Morita, and T. Iida, *J. Phys. Condens. Matter* **6**, 811 (1994).